

## Rotational Damping in Ytterbium Nuclei

F. S. Stephens, M. A. Deleplanque, I. Y. Lee, D. Ward, P. Fallon, M. Cromaz, R. M. Clark, R. M. Diamond, A. O. Macchiavelli, and K. Vetter

*Nuclear Science Division, Lawrence Berkeley National Laboratory, Berkeley, California 94720*

(Received 19 October 2001; published 20 March 2002)

We have made the first clear measurements of rotational damping widths in nuclei. In a mixture of three Yb nuclei, these widths are  $300 \pm 60$  keV between 1.2 and 1.5 MeV  $\gamma$ -ray energy [ $\sim(37-57)\hbar$ ]. Compound damping and motional narrowing are discussed in connection with these results.

DOI: 10.1103/PhysRevLett.88.142501

PACS numbers: 21.10.Re, 23.20.Lv, 27.60.+j, 27.70.+q

When as little as 1 MeV of thermal energy is added to rotational nuclei, like those studied here, the level separations become very small and the levels mix. This process is the damping of the nucleonic motion from ordered to chaotic, a very interesting subject. However, the same high level density that induces the mixing causes the emitted  $\gamma$ -ray spectra to consist of very many lines, currently unresolvable, making studies difficult. Nevertheless, some observables have been proposed. If all the nearby bands had very similar rotational properties, the mixed bands would have these same properties; a situation proposed but not yet observed [1]. In general, the initial bands have different rotational properties and in this case unmixed levels of the same spin emit rotational  $\gamma$  rays of different energies (or frequencies) and the mixed levels can emit  $\gamma$  rays having any of these energies. This “rotational damping” is an important change because a level of spin  $I$  no longer decays to a single level of spin  $I - 2$  but to any of a number of levels. The resulting distribution of  $\gamma$ -ray energies emitted by a single level has a FWHM that is called the “rotational damping width” ( $\Gamma_{\text{rot}}$ ). Attempts to measure  $\Gamma_{\text{rot}}$  began about 15 years ago [2,3], and shortly thereafter very rough values in the correct (presently measured) range were reported [4,5].

One way to study rotational damping is to look at correlations in the spectrum in coincidence with a given  $\gamma$ -ray energy (the gate). Such spectra show the relative likelihood that  $\gamma$  rays are associated with the gating  $\gamma$  rays. In an undamped rotational band the emitted  $\gamma$ -ray energies are roughly proportional to the spins, and therefore the decay of a high-spin state consists of a sequence of approximately equally spaced lines with monotonically decreasing energies (like a picket fence). A gate on one of these  $\gamma$  rays will be in coincidence with all the others, but not with itself. This generates a strong negative correlation at the gate energy in the gated spectrum, called the “rotational” correlation, which has an area of exactly one transition, the missing gate. Even if the initial spectrum consists of a superposition of many undamped rotational bands having different properties (moments of inertia and alignments), a gate at a given energy would produce such a rotational correlation, although the shape would depend slightly on the properties of the superposed bands. Rotational damping,

however, modifies this behavior. The missing transition is no longer a sharp line, but has a shape that reflects the distributions of  $\gamma$ -ray energies emitted by the levels that contribute to the gate. Previous studies have found the rotational correlations corresponding to superpositions of “undamped” bands [2,3], but not those from rotationally damped bands. We have found that the rotational correlation from damped bands is masked by a positive “feeding” correlation, which we can remove. This reveals for the first time the shape of the one missing transition.

The data were taken using Gammasphere [6] at the LBNL 88-Inch Cyclotron to record  $\gamma$  rays from the reaction of 215 MeV  $^{48}\text{Ca}$  projectiles on a 1 mg/cm<sup>2</sup> target of  $^{124}\text{Sn}$ . This reaction forms the fusion product,  $^{172}\text{Yb}$ , which decays into the product nuclei,  $^{168,167,166}\text{Yb}$ , with yields of roughly 20%, 40%, and 40%, respectively. Events were stored if 5-or-more clean (no hit in the Compton suppressor)  $\gamma$  rays were in coincidence. About  $2 \times 10^9$  such events were recorded and sorted into a 2D ( $E_\gamma$ - $E_\gamma$ ) matrix. A second set of data (called the “multiplicity” measurement) was taken using ATLAS at ANL with the same bombarding conditions and trigger, but with the Gammasphere hevimet collimators removed in order to measure the total number of  $\gamma$ -ray hits for each event.

The correlation (COR) spectra were generated from the 2D matrix using the COR procedure [7] which subtracts an uncorrelated background from the data. For a gated spectrum this background is the full-projection spectrum normalized to the area of the gated spectrum. It is often useful to “renormalize” the background spectrum to the area of a (“fully fed”) region in the spectrum through which all the feeding passes,  $\sim 650$ – $800$  keV in our case.

We have generated a simplified simulation matrix to illustrate the correlations. This simulation has a perfect rotor with transition energies 64 keV apart, a Gaussian E2 strength function with a  $\Gamma_{\text{rot}}$  of 80 keV, and a constant feeding intensity between 1.0 and 1.7 MeV (about  $30\hbar$  to  $55\hbar$ ). The essential features are similar to those of the real spectra except that  $\Gamma_{\text{rot}}$  is smaller to make it easier to see. Figure 1a shows spectra having a 20-keV wide gate at 600 keV. The feeding range is clear in these spectra and the 600 keV gate is fully fed. The rotational correlation is

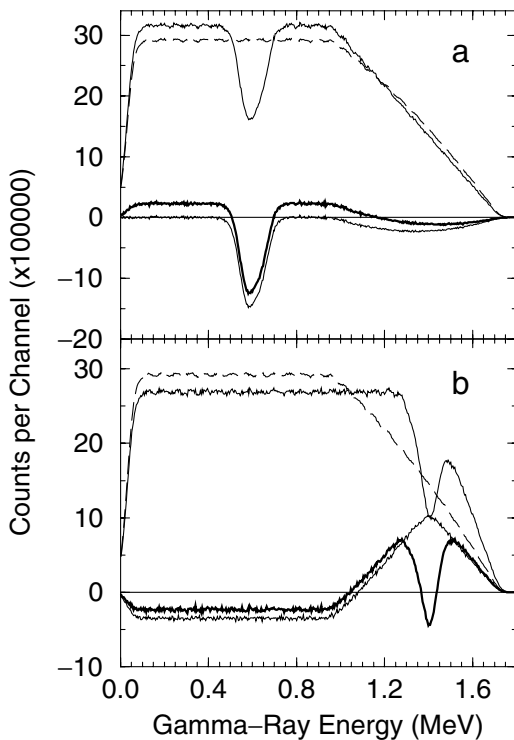


FIG. 1. Spectra from the simplified simulation: (a) 600 keV gate; (b) 1400 keV gate. Upper light lines, gated spectra; dashed lines, uncorrelated backgrounds; heavy lines, CORs; lower light lines, (a) renormalized COR, (b) feeding COR.

preserved exactly in both the COR and renormalized COR spectrum. There is a shallow dip in the feeding range of the (renormalized) COR spectrum, called the “secondary feeding correlation,” from which the location and shape of the feeding can be derived [8].

Figure 1b shows spectra gated in the feeding range at 1.4 MeV. The rotational correlation is clear in the COR spectrum, but is superposed on a large positive correlation which we call the (primary) “feeding correlation.” In rotational nuclei, a gate in the feeding range is most correlated with the transitions immediately above and below itself (i.e., having almost the same feeding). As the coincident  $\gamma$ -ray energy (spin) gets farther from the gate energy, there will be more feeding that produces one but not the other, resulting in a lower correlation. We can see this feeding correlation directly by using a “feeding simulation” that, without changing anything else, allows the rotational  $\gamma$ -ray gate to be in coincidence with itself (i.e., with a second  $\gamma$  ray selected using exactly the same constraints), thereby removing the rotational correlation. The feeding correlation is also shown in Fig. 1b, where it is clear that subtracting it from the normal correlation spectrum will leave just the rotational correlation, and renormalization will make the subtraction more accurate. This is the procedure we will use on the experimental data.

The realistic simulation code [9] consists of separate cascades of rotational and statistical  $\gamma$  rays, whereas in nuclei there is a single competitive cascade. The cascades

themselves are not likely to be significantly affected by treating them separately; however, some problems arise as discussed later. The statistical cascade starts at an excitation energy selected (randomly) from a Gaussian of FWHM 0.5 MeV centered around a thermal excitation energy of 8 MeV (the approximate neutron binding energy) and ends when the excitation energy becomes less than 0.4 MeV. The spectrum of statistical  $\gamma$  rays has the form,  $N_\gamma \sim E_\gamma^3 \exp(-E_\gamma/T)$ , where  $T$  is the average temperature. These  $\gamma$  rays are uncorrelated and thus not very important for the present results.

The rotational cascade starts from a spin selected from an input feeding table (Fig. 2a). A change from damped to “undamped” bands is expected [10] to occur around a thermal excitation energy of about 0.75 MeV, which corresponds on average [11] to a spin about  $30\hbar$  and  $\gamma$  rays of about 1 MeV. Without a competitive cascade this change does not come automatically, so we input a table giving the amount of jumping from the damped bands to the “undamped” bands for each spin. In the damped bands the  $\gamma$ -ray energy is read from a table (Fig. 2b) and incremented by an amount selected from a Gaussian distribution centered at zero whose width is the input  $\Gamma_{\text{rot}}$  for that spin. Since  $\Gamma_{\text{rot}}$  is also a function of the thermal excitation energy, we measure “effective” damping widths corresponding to an average thermal excitation energy at each spin. The response function of Gammasphere was determined with  $\gamma$ -ray sources and used in all the simulations. For each cascade, pairs of  $\gamma$  rays were incremented into a 2D matrix, which was then treated exactly like the data.

The “undamped”  $\gamma$  rays have little effect on the energy region studied here where they comprise at most about 10% of one transition. In the data there is a narrow dip (with small ridges) at the gate energy for gates below about 1.3 MeV, and we attribute these to “undamped” population. In our simulation each “undamped” band has its spins incremented with a spin “alignment” selected from a Gaussian distribution centered at zero with a FWHM of  $2\hbar$ . The energy from Fig. 2b for the resultant spin is then incremented with that selected from a 40 keV damping width (see above). This small damping width is needed to reduce the ridge intensity near the narrow dip so that it resembles the data, and we did not find any other reasonable way to do this. Recent studies [12–14] suggest there may be a second type of damping in rotational nuclei, called compound damping, which arises from the spread in energy of the basis states due to their mixing. The effects of this compound damping are expected to be largest as the mixing sets in and to become small when it involves many levels. Our 40-keV damping width is about the right size to represent an average compound damping but small enough to retain the general features of undamped bands. Thus our “undamped” bands include both types of band, and we do not try to separate them here. In this work we have avoided gate energies below 1.2 MeV where “undamped” effects become larger and our description less reliable.

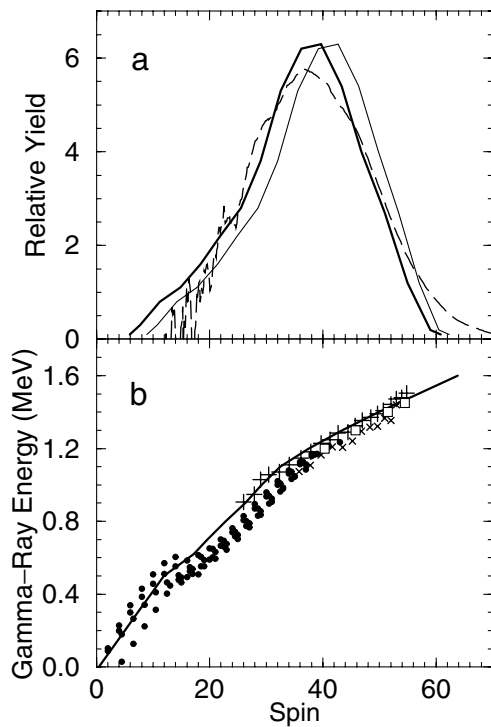


FIG. 2. Simulation inputs: (a) feeding; (b)  $\gamma$ -ray energies.

The light line in Fig. 2a is the feeding as a function of spin determined from the multiplicity measurement. The total number of  $\gamma$ -ray hits was converted into multiplicities and then into spins using the Gammasphere response function and the angular distributions of the  $\gamma$  rays [15]. The dashed curve is obtained from the secondary feeding correlation referred to above. The heavy line is the input used, where we have taken the shape from the multiplicity measurement and the location from the secondary feeding correlation.

The input  $\gamma$ -ray energies are shown in Fig. 2b. The dots are the lowest positive- and negative-parity discrete bands in each of the three product nuclei. These are extended up in spin by the squares, which are based on the measured dynamic moment-of-inertia values [16]. The pluses and crosses are recent values from multiplicity measurements [15] on the unresolved regions of the spectrum. The crosses are from data taken on the  $8\pi$  spectrometer and the pluses are from the Gammasphere data used in this study. As the input we use the line, which weights the present Gammasphere data most heavily and reproduces well the full  $\gamma$ -ray spectrum.

The results of this study are shown in Fig. 3, where all the gates are 20 keV wide and the spectra are CORs normalized to the same number of counts in every gate. The overall agreement between the simulations and the data is good, and variation of the inputs shows that it is reasonably robust. The population of the narrow dips is controlled by the jumping probabilities from damped to “undamped” bands which were adjusted *ad hoc* to give reasonable fits to

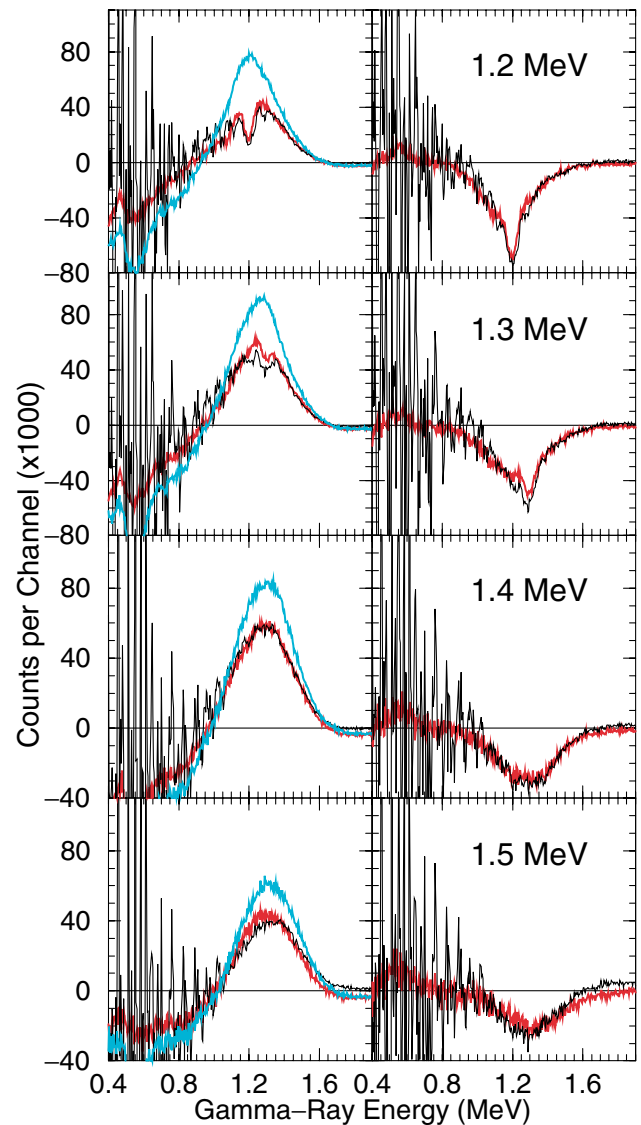


FIG. 3. The black, red, and blue lines are COR spectra (left) and differences (right) for the data, simulations, and feeding simulations, respectively, at four gate energies.

the data. This probability is 2%–3% per state from  $\sim 50\hbar$  down to  $\sim 30\hbar$  (which includes the narrow dips seen here), below which it increases rapidly. There are peaks in the data between  $\gamma$ -ray energies 0.7 and 1.0 MeV that persist for all gates. This indicates the preferential population of “quasi-identical” bands, which presumably involve an energetically favorable nucleon (intruder) configuration that dominates the near-yrast bands. Many known discrete bands contribute to these peaks and a damped component cannot be excluded at present. Our simulations are typically too low in this region, causing the simulated widths to be slightly larger than those of the data.

The feeding correlations in Fig. 3 are subtracted from the other COR spectra (renormalized difference) in order to isolate the rotational correlations, which are shown in Fig. 3 (right side) for both the data and the simulations.

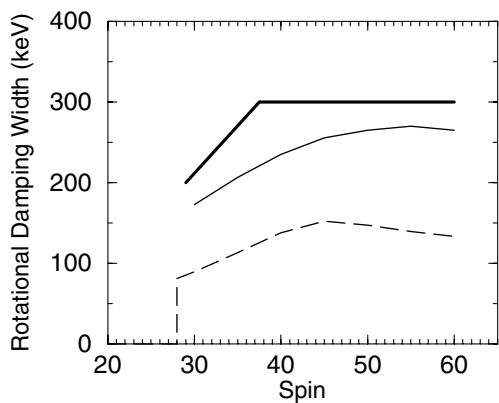


FIG. 4. The heavy line shows the  $\Gamma_{\text{rot}}$  values from this work. The light solid and dashed lines show the calculations of Matsuo *et al.* [12] and Lauritzen *et al.* [10], respectively.

The areas of the experimental and simulated rotational correlations are the same in all the cases, indicating that there is one ( $1.0 \pm 0.1$ ) transition missing in the data, since that must be the case in the simulation. The shapes of the correlations for the 1.2 and 1.3 MeV gates are fit well by two Gaussians. We associate the wide Gaussian with rotational damping, while the narrow one we have called “undamped” and discussed above. The shapes of the correlations for the 1.4 and 1.5 MeV gates are well fit by single Gaussians.

The shape of the missing transition is affected by the presence of overlapping (damped) transitions from several different spins in the gate. Transitions from each of these spins reflect their own shape in the missing gate, thereby increasing its width and affecting its shape. This limits the information obtained about the shape of the primary distribution of  $\gamma$  rays emitted by states of a single spin. Our fits are sensitive to the width  $\Gamma_{\text{rot}}$  (actually to the second moment) of the primary distribution, but it is not yet clear what can be said about the higher moments. The E2 strength function from a state should be similar to this primary distribution, but may differ somewhat due to the spread in  $\gamma$ -ray energies and level densities. The values for  $\Gamma_{\text{rot}}$  are the simulation inputs, which are 300 keV for these gates (see Fig. 4). Simulations with varying inputs and  $\Gamma_{\text{rot}}$  values show that the uncertainty limits on  $\Gamma_{\text{rot}}$  are about  $\pm 20\%$ .

The heavy line in Fig. 4 shows the  $\Gamma_{\text{rot}}$  values determined from our analysis. Rotational damping widths were first calculated by Lauritzen *et al.* [10], who give analytical formulas for both the rotationally damped and the motionally narrowed regions. Motional narrowing sets in when the region over which levels are mixed becomes comparable with  $\Gamma_{\text{rot}}$ . The dashed line shows the effective damping width from the Lauritzen calculations. To get this curve we used thermal excitation energies for each spin

from the asymptotic pathway for the  $\gamma$ -ray decay given by Døssing and Vigezzi [11]. We also received effective  $\Gamma_{\text{rot}}$  values from Vigezzi *et al.* [17] that are based on the cranking calculations of Matsuo *et al.* [12] and these are shown as the light line in Fig. 4. The much larger values from the Matsuo calculations are presumably due to shell effects. That the data are 20% larger than the cranking-model estimate is near our uncertainty limit but also might be due to variations in the strong shell effects present in the Matsuo calculations.

There may be some effects due to motional narrowing in our results. The contribution of motional narrowing can be evaluated in the Lauritzen calculations where the flatness of  $\Gamma_{\text{rot}}$  above about  $40\hbar$  comes from higher values, normally expected with increasing spin and excitation energy, offset by lowered values due to motional narrowing. However, in this calculation, the damping widths are much lower than the experimental values. In the cranking-model results the flatness seems more likely to be due to the shell effects, but these calculations may not go to high enough thermal excitation energies. To clarify this situation, a better determination of the thermal excitation energies involved for the highest spins is needed, together with cranking-model results for this range.

We measured the first clear  $\Gamma_{\text{rot}}$  values in nuclei. The narrow dips and ridges that we see seem to be explained by a mixture of undamped bands and compound-damped bands. The failure of  $\Gamma_{\text{rot}}$  to increase with increasing spin at the highest spins may involve motional narrowing.

We thank E. Vigezzi and B. Herskind for valuable discussions. This work has been supported in part by the U.S. DOE under Contract No. DE-AC03-76SF00098.

- 
- [1] B. R. Mottelson, Nucl. Phys. **A557**, 717c (1993).
  - [2] J. C. Bacelar *et al.*, Phys. Rev. Lett. **55**, 1858 (1985).
  - [3] J. E. Draper *et al.*, Phys. Rev. Lett. **56**, 309 (1986).
  - [4] F. S. Stephens *et al.*, Phys. Rev. Lett. **57**, 2912 (1986).
  - [5] F. S. Stephens *et al.*, Phys. Rev. Lett. **58**, 2186 (1987).
  - [6] I. Y. Lee, Nucl. Phys. **A520**, 641c (1990).
  - [7] O. Andersen *et al.*, Phys. Rev. Lett. **43**, 687 (1979).
  - [8] F. S. Stephens *et al.* (to be published).
  - [9] I. Y. Lee (to be published).
  - [10] B. Lauritzen, T. Døssing, and R. A. Broglia, Nucl. Phys. **A457**, 61 (1986).
  - [11] T. Døssing and E. Vigezzi, Nucl. Phys. **A587**, 13 (1995).
  - [12] M. Matsuo *et al.*, Nucl. Phys. **A649**, 379c (1999).
  - [13] S. Leoni *et al.*, Nucl. Phys. **A587**, 513 (1995).
  - [14] T. Døssing *et al.*, Acta Phys. Pol. B **32**, 2565 (2001).
  - [15] D. Ward *et al.* (to be published).
  - [16] M. A. Deleplanque *et al.*, Nucl. Phys. **A448**, 495 (1985).
  - [17] E. Vigezzi, S. Leoni, and M. Matsuo (private communication).